the H_2 reductive-elimination process of importance to homogeneous and heterogeneous hydrogenation catalysis, the isotope effect observed supports the model of a late transition state where the H–H bond forms nearly completely either in the transition state or in a metastable η^2-H_2 intermediate. The relatively low (10–20 kcal/mole) enthalpies of activation for hydrogen reductive elimination for these late metal dihydrides emphasize the small energy difference between the dihydride, η^2-dihydrogen, and free dihydrogen structures. The high stability of platinum(II) dihydrides that contain bulky phosphine ligands must derive primarily from kinetic stability. Our results show that hydrogen reductive elimination is surprisingly solvent sensitive, with the dihydride complex being kinetically stabilized in polar-coordinating solvents. Invoking the principle of microscopic reversibility allows this solvent effect to be viewed in another context. Addition of molecular hydrogen to form a *cis*-dihydride complex must involve some charge separation, and polar solvents might aid in stabilizing dihydride formation.

The similarity between the isotope effects for dihydrogen reductive elimination, and those observed recently[15,46] for alkane elimination from late metal centers, suggests a similarity in the reverse processes of hydrogen and hydrocarbon activation. Crucial to the success of these reactions will be the proper η^2-orientation of the C–H or H–H bond so that the transition state for oxidative addition can be reached. Thus, aside from the thermodynamic constraints,[61,62] the kinetic limitations to C–H activation[15] may arise from steric barriers to achieving the η^2-precursor geometry. Indeed in late metal systems, where there is evidence for concerted C–H oxidative addition,[47] tertiary C–H groups in hydrocarbons show no reactivity.

Acknowledgment. This material is based on work supported by the National Science Foundation (Grant CHE-8504088). We thank Johnson Matthey for a sample of K_2PtCl_4 under their metal loan program. We thank Charles L. Perrin, Tammy Dwyer, and John Thoburn for assistance with spin-saturation-transfer experiments and with spectral simulations.

Registry No. $PtH_2(PMe_3)_2$, 103530-01-4; $PtH_2(PMe_3)_3$, 113705-04-7; Me_3P, 594-09-2; D_2, 7782-39-0.

Contribution from the School of Chemical Sciences,
University of Illinois at Urbana-Champaign, Urbana, Illinois 61801

Synthesis and Characterization of Coordinately Unsaturated Phosphine Complexes of Divalent V, Cr, Mn, Fe, and Co. Crystal Structures of $[CrCl_2(dippe)]_2$ and $FeCl_2(dippe)$

Ann R. Hermes and Gregory S. Girolami*

Received December 4, 1987

The reaction of divalent transition-metal halides with the bulky chelating phosphine 1,2-bis(diisopropylphosphino)ethane, dippe, gives a series of coordinately unsaturated complexes of stoichiometry $MX_2(dippe)$ for M = V, Cr, Mn, Fe, or Co. Both the vanadium(II) and chromium(II) complexes readily form adducts with tetrahydrofuran or acetonitrile. The base-free chromium species exists as a dimer in the solid state, $[CrCl_2(dippe)]_2$, that consists of two square-planar chromium centers arranged in pairs via asymmetric chloride bridges. Averaged distances for the two independent molecules are as follows: Cr···Cr = 3.605 (2) Å; Cr–P = 2.481 (2), 2.511 (2) Å; Cr–Cl(t) = 2.333 (2) Å; Cr–Cl(b) = 2.380 (2), 2.606 (2) Å. Crystal data for $Cr_2Cl_4P_4C_{28}H_{64}$: space group $P\bar{1}$, $a = 13.225$ (2) Å, $b = 14.834$ (3) Å, $c = 11.101$ (2) Å, $\alpha = 97.35$ (1)°, $\beta = 114.21$ (1)°, $\gamma = 84.26$ (1)°, $V = 1967.3$ (6) Å^3, $Z = 2$, $R_F = 4.2\%$, $R_{wF} = 4.7\%$ on 3435 reflections and 344 variables. The manganese, iron, and cobalt complexes are all tetrahedral monomers, as confirmed by the X-ray crystal structure of $FeCl_2(dippe)$: Fe–P = 2.46 (1) Å, Fe–Cl = 2.21 (1) Å, P–Fe–P = 83.8 (3)°, Cl–Fe–Cl = 117.1 (4)°. Crystal data for $FeCl_2P_2C_{14}H_{32}$: space group *Pbca*, $a = 24.66$ (1) Å, $b = 22.67$ (1) Å, $c = 14.995$ (6) Å, $V = 8385$ (8) Å^3, $Z = 16$, $R_F = 12.0\%$, $R_{wF} = 12.6\%$ on 1547 reflections and 201 variables. NMR and EPR studies show that all of the four-coordinate species exist in high-spin electronic configurations. The $MX_2(dippe)$ complexes provide an excellent opportunity to examine the behavior of coordinately unsaturated first-row transition-metal species and serve as excellent starting materials for the preparation of low-electron-count organometallic derivatives of these elements.

Introduction

There are few areas of inorganic chemistry in which research activity is as great as the study of transition-metal complexes that contain phosphine ligands.[1,2] Organophosphines are able to stabilize metals in a wide variety of oxidation states and are unequaled as attendant ligands in many homogeneous catalytic processes.[3] The usefulness and versatility of phosphine ligands arise in part from their ability to engage in synergistic σ-donor and π-acceptor interactions with metal atoms and also from the chemist's ability to vary these electronic properties in a systematic fashion. The steric parameters of an organophosphine ligand can likewise be varied over a large range, essentially independently of its electronic properties.[4] Accordingly, the coordination number, coordination geometry, electron richness of a metal center, and the thermodynamics and kinetics of associative and dissociative equilibria can be tailored almost at will by a judicious choice of the substituents on phosphorus.

Our research is directed toward the preparation and study of coordinately unsaturated metal complexes, particularly of the early first-row transition elements.[5-13] Our approach is to employ phosphine ligands possessing appropriately selected electronic and steric properties that stabilize molecules in which the transition metal adopts an unusual electron count, coordination geometry, or oxidation state. Such species are expected to exhibit enhanced reactivity compared with that of coordinately saturated analogues.

The large atomic radii and the relatively electropositive nature of low-valent early transition elements suggest that electron-donating phosphines should best serve as ligating groups. Previous

---

(1) McAuliffe, C. A. *Transition Metal Complexes of Phosphorus, Arsenic, and Antimony Ligands*; Macmillan: New York, 1973.

(2) McAuliffe, C. A.; Levason, W. *Phosphine, Arsine and Stibine Complexes of the Transition Elements*; Elsevier: New York, 1979.

(3) Pignolet, L. H. *Homogeneous Catalysis with Metal Phosphine Complexes*; Plenum: New York, 1983.

(4) Tolman, C. A. *Chem. Rev.* **1977**, *77*, 313.

(5) Jensen, J. A.; Girolami, G. S. *J. Chem. Soc., Chem. Commun.* **1986**, 1160.

(6) Hermes, A. R.; Girolami, G. S. *Organometallics* **1987**, *6*, 763.

(7) Hermes, A. R.; Girolami, G. S. *Organometallics* **1988**, *7*, 394.

(8) Jensen, J. A.; Girolami, G. S. *J. Am. Chem. Soc.*, in press.

(9) Morris, R. J.; Girolami, G. S. *Organometallics* **1987**, *6*, 1815.

(10) Gardner, T. G.; Girolami, G. S. *Organometallics* **1987**, *6*, 2551.

(11) Gardner, T. G.; Girolami, G. S. *J. Chem. Soc., Chem. Commun.* **1987**, 1758.

(12) Hermes, A. R.; Morris, R. J.; Girolami, G. S., submitted for publication in *Organometallics*.

(13) Jensen, J. A.; Wilson, S. R.; Schultz, A. J.; Girolami, G. S. *J. Am. Chem. Soc.* **1987**, *109*, 8094.

0020-1669/88/1327-1775$01.50/0

Table I. Physical and Microanalytical Data for the New $MX_2(dippe)$ Complexes

compd	color	mp/°C	% calcd C	% calcd H	% calcd X	% found C	% found H	% found X
$VBr_2(dippe)\cdot{}^3/_2thf$	green	>250	41.3	7.70	27.5	41.7	7.61	27.6[a]
$[CrCl_2(dippe)]_2$	blue	>250	43.6	8.37	18.4	42.7	8.33	17.9
$[CrBr_2(dippe)]_2$	blue	>250	35.5	6.80	33.7	35.3	7.08	33.7
$CrBr_2(dippe)\cdot MeCN$	blue	>250	37.3	6.85	31.1	37.1	7.19	31.7[b]
$MnCl_2(dippe)$	pale green	150	43.3	8.31	18.4	43.5	8.33	18.5
$MnBr_2(dippe)$	pale green	128–129	35.2	6.76	33.5	35.3	6.72	33.5
$MnI_2(dippe)\cdot PhMe$	pale orange	84–86	36.2	6.08	38.3	35.5	5.86	39.2
$FeCl_2(dippe)$	lavender	142–143	44.3	8.29	18.2	42.7	8.35	18.6
$FeBr_2(dippe)$	orange-brown	123–125	35.2	6.75	33.4	35.3	6.88	33.8
$FeI_2(dippe)$	olive green	218–220	29.4	5.64	44.4	29.2	5.78	44.9
$CoCl_2(dippe)$	blue-green	185–188	42.9	8.23	18.1	42.7	8.35	18.1

[a] V: calcd, 8.8; found, 9.3. [b] N: calcd, 2.72; found, 2.77.

work has shown that the phosphine ligand 1,2-bis(dimethylphosphino)ethane, dmpe, gives octahedral diadducts with metal dihalides of stoichiometry $MX_2(dmpe)_2$.[14-16] In order to obtain adducts that are substantially more coordinately unsaturated, it is of interest to investigate more sterically demanding phosphines that would reduce the coordination number to less than 6. Initial studies with bulky unidentate phosphines such as $P(t\text{-Bu})_3$ were not encouraging, so chelating phosphines were investigated in order to improve the stability of the complexes. Accordingly, the coordination chemistry of the bidentate phosphine 1,2-bis(diisopropylphosphino)ethane, dippe, with the divalent halides of vanadium, chromium, manganese, iron, and cobalt is now described. The sterically bulky isopropyl substituents do in fact limit the coordination number (and thus the electron count) of the adducts. These coordinately unsaturated species are of interest in their own right; they also serve as excellent starting materials for the investigation of low-valent organometallic complexes of the early first-row metals.[6,12]

Results and Discussion

Vanadium(II). The vanadium salt $[V_2Cl_3(thf)_6]_2[Zn_2Cl_6]$[17,18] has proven useful as a starting material for a number of divalent vanadium species, including the phosphine complex $VCl_2(dmpe)_2$.[16] However, addition of dippe to the vanadium salt led under various conditions to intractable green oils that retained zinc and could not be purified. A successful route to vanadium(II) phosphine complexes was developed by reduction of $VBr_3(thf)_3$, thf = tetrahydrofuran, with magnesium in the presence of dippe to give a green crystalline compound of stoichiometry $VBr_2(dippe)\cdot{}^3/_2thf$ (**1**). Elemental analysis confirms the lack of magnesium in the product.

$$VBr_3(thf)_3 + {}^1/_2Mg + dippe \rightarrow VBr_2(dippe)\cdot{}^3/_2thf + {}^1/_2MgBr_2 + {}^3/_2thf$$

1

This preparative method is similar to the reductive synthesis of $Cp_2V_2Cl_2(PEt_3)_2$ from $CpVCl_2(PEt_3)_2$.[19] The IR spectrum of **1** shows bands at 1031 and 881 cm^{-1} due to coordinated thf. The +2 oxidation state of **1** was confirmed by treatment with 2 equiv of dmpe, which gives the octahedral species $VBr_2(dmpe)_2$; this complex is analogous to the known chloro derivative $VCl_2(dmpe)_2$.[16] Given the stoichiometry and the strong tendency of vanadium(II) to adopt octahedral geometries, the structure of the dippe adduct is most likely related to that of $Cp_2V_2Cl_2(PEt_3)_2$,[19] viz., a chloride-bridged dimer with a V···V separation of over 3.0 Å. Evidently, both coordinated thf and lattice thf are present in the crystalline solid. Unfortunately, the poor solubility of the complex has prevented characterization by NMR spectroscopy, and the crystals are unsuited for structure determination by X-ray crystallography. Nevertheless, **1** is important as a rare example of divalent vanadium.

The chemistry of vanadium in its lower oxidation states is still poorly characterized, and the lack of good starting materials is in large part responsible for this fact. The previously mentioned zincate salt $[V_2Cl_3(thf)_6]_2[Zn_2Cl_6]$ has been used to prepare other low-valent vanadium species; however, the low solubility in organic solvents and the complicating presence of zinc makes this species of only occasional utility as a starting material. The phosphine adduct **1** may be a useful starting material for the preparation of other low-valent complexes of vanadium.

Few other phosphine adducts of vanadium(II) are known. The green adducts "$VCl_2(PEt_3)_2$" and $V(thf)_2[ZnCl_3(PPh_3)]_2$ have been prepared[20,21] by addition of PR_3 to $[V_2Cl_3(thf)_6]_2[Zn_2Cl_6]$, while reaction of an analogous divanadium cation with PMe_3 has led to the red species $[V_2Cl_3(PMe_3)_6][AlEt_2Cl_2]$.[22] The dimeric vanadium(II) borohydride $V_2Cl_2(BH_4)_2(dppm)_2$[23] and the porphyrin complex $V(oep)(PMe_2Ph)_2$[24] are also known. The only well-characterized monomeric adduct of a vanadium(II) halide with a phosphine ligand is $VCl_2(dmpe)_2$.[16] Vanadium(II) complexes are of interest as potential catalysts for the polymerization of ethylene.[25]

Chromium(II). Addition of dippe to the chromium(II) halides $CrCl_2(thf)$ or $CrBr_2(thf)_2$ rapidly gives blue ether solutions from which complexes of stoichiometry $CrX_2(dippe)$ precipitate. These "base-free" complexes are only sparingly soluble in hydrocarbons but may be recrystallized from hot toluene to give X-ray-quality crystals. The infrared spectrum of the chloride complex contains ν_{CrCl} bands at 300 and 270 cm^{-1}.

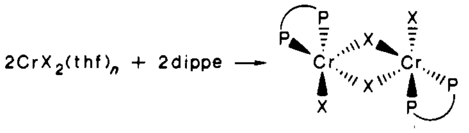

2a, X = Cl
b, X = Br

Complexes **2a** and **2b** are very soluble in strongly coordinating solvents such as acetonitrile, and the magnetic moment of 5.0 μ_B in acetonitrile is consistent with the presence of a high-spin d^4 metal center. Recrystallization of **2b** from acetonitrile yields blue prisms of the adduct $CrBr_2(dippe)\cdot CH_3CN$; this complex possesses in-

---

(14) Girolami, G. S.; Salt, J. E.; Wilkinson, G.; Thornton-Pett, M.; Hursthouse, M. B. *J. Am. Chem. Soc.* **1983**, *105*, 5954.

(15) Girolami, G. S.; Wilkinson, G.; Thornton-Pett, M.; Hursthouse, M. B. *J. Am. Chem. Soc.* **1983**, *105*, 6752.

(16) Girolami, G. S.; Wilkinson, G.; Thornton-Pett, M.; Hursthouse, M. B. *J. Chem. Soc., Dalton Trans.* **1985**, 1339.

(17) Bouma, R. J.; Teuben, J. H.; Beukema, W. R.; Bansemer, R. L.; Huffman, J. C.; Caulton, K. G. *Inorg. Chem.* **1984**, *23*, 2715.

(18) Cotton, F. A.; Duraj, S. A.; Roth, W. J. *Inorg. Chem.* **1985**, *24*, 913.

(19) Nieman, J.; Teuben, J. H.; Huffman, J. C.; Caulton, K. G. *J. Organomet. Chem.* **1983**, *225*, 193.

(20) Hall, V. W.; Schmulbach, C. D.; Soby, W. N. *J. Organomet. Chem.* **1981**, *209*, 69.

(21) Cotton, F. A.; Duraj, S. A.; Roth, S. J.; Schmulbach, C. D. *Inorg. Chem.* **1985**, *24*, 525.

(22) Cotton, F. A.; Duraj, S. A.; Manzer, L. E.; Roth, W. J. *J. Am. Chem. Soc.* **1985**, *107*, 3850.

(23) Cotton, F. A.; Duraj, S. A.; Roth, W. J. *Inorg. Chem.* **1984**, *23*, 4113.

(24) Poncet, J. L.; Barbe, J.-M.; Guilard, R.; Oumous, H.; Lecomte, C.; Protas, J. *J. Chem. Soc., Chem. Commun.* **1982**, 1421.

(25) Smith, P. D.; Martin, J. L.; Huffman, J. C.; Bansemer, R. L.; Caulton, K. G. *Inorg. Chem.* **1985**, *24*, 2997.

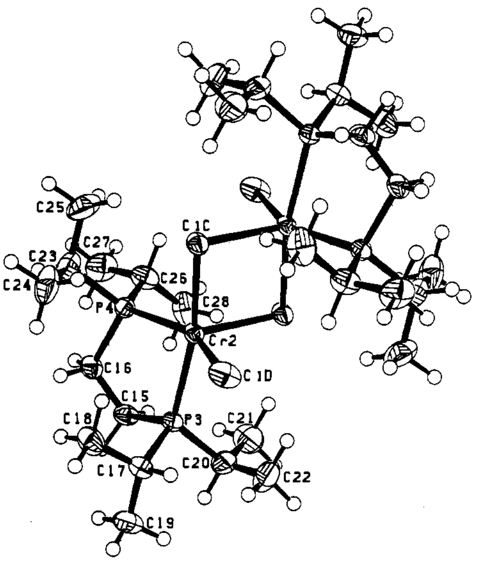

Figure 1. Molecular structure of $[CrCl_2(dippe)]_2$. Molecule 2 is shown; molecule 1 adopts an essentially identical structure.

Table II. Crystal Data for $[CrCl_2(dippe)]_2$ and $FeCl_2(dippe)$ (25 °C)

	$Cr_2Cl_4P_4C_{28}H_{64}$	$FeCl_2P_2C_{14}H_{32}$
space group	$P\bar{1}$	*Pbca*
a/Å	13.225 (2)	24.66 (1)
b/Å	14.834 (3)	22.67 (1)
c/Å	11.101 (2)	14.995 (6)
α/deg	97.35 (1)	90
β/deg	114.21 (1)	90
γ/deg	84.26 (1)	90
V/Å^3	1967.3 (6)	8385 (8)
Z	2	16
mol wt	770.52	389.11
d_{calcd}/g cm^{-3}	1.301	1.233
μ_{calcd}/cm^{-1}	9.91	11.16
size/mm	0.2 × 0.3 × 0.3	0.3 × 0.3 × 0.5
diffractometer	Syntex $P2_1$	
radiation	Mo K$\bar{\alpha}$, $\bar{\lambda}$ = 0.71073 Å	
monochromator	graphite crystal	
scan range	$3.0 \leq 2\theta \leq 46.0°$	
scan speed, type	4–20° min^{-1}, $\omega/2\theta$	
no. of reflcns, total	6045	6690
no. of reflcns, unique	5444	5857
no. of reflcns, $I > 2.58\sigma(I)$	3435	1547
R_i/%	1.7	
R_F/%	4.2	12.0
R_{wF}/%	4.7	12.6
variables	344	201
p factor	0.020	0.030

frared bands at 2313 and 2278 cm^{-1} that are indicative of coordinated acetonitrile (free acetonitrile has a combination band at 2297 cm^{-1} and its C≡N stretch at 2257 cm^{-1}).[26] The ready formation of a five-coordinate acetonitrile adduct is consistent with the coordination geometry observed in the X-ray crystal structure of the base-free form of $CrCl_2(dippe)$.

The X-ray crystal structure of **2a** reveals that the base-free chromium complex adopts a *dimeric* structure, $[CrCl_2(dippe)]_2$, in the solid state. An ORTEP diagram of the molecular structure is given in Figure 1, and crystal data are given in Table II. Final atomic coordinates and selected bond distances and angles are presented in Tables III and IV.

The $[CrCl_2(dippe)]_2$ molecules are arranged on centers of symmetry that bisect the Cr···Cr vector; the two crystallographically independent molecules in the unit cell have very similar bond lengths and angles. The structure is best regarded as being composed of square-planar $CrCl_2(dippe)$ units that are rather loosely bound in pairs via weak axial chloride interactions. With the inclusion of the weak chloride bridges, the chromium centers are accordingly five-coordinate and adopt distorted square-pyramidal geometries. This type of bonding has been noted in some other square-planar chromium(II) species, such as $Cr(acac)_2$,[27]

Table III. Final Atomic Coordinates for $[CrCl_2(dippe)]_2$

	x/a	y/b	z/c
Cr1	0.9037 (7)	0.52793 (6)	0.33393 (8)
Cr2	0.35730 (7)	−0.02539 (6)	−0.06207 (8)
ClA	0.9021 (1)	0.42422 (9)	0.4779 (1)
ClB	0.9713 (1)	0.4181 (1)	0.2078 (2)
ClC	0.4539 (1)	0.08133 (9)	−0.1122 (1)
ClD	0.2954 (1)	0.0819 (1)	0.0692 (2)
P1	0.8766 (1)	0.6379 (1)	0.1692 (2)
P2	0.7581 (1)	0.6304 (1)	0.3710 (2)
P3	0.2315 (1)	−0.1348 (1)	−0.0534 (2)
P4	0.3322 (1)	−0.1250 (1)	−0.2725 (2)
C1	0.7666 (7)	0.7230 (5)	0.1714 (8)
C2	0.7097 (6)	0.7130 (5)	0.2469 (7)
C3	0.8302 (5)	0.5884 (4)	−0.0032 (6)
C4	0.7340 (6)	0.5284 (5)	−0.0404 (7)
C5	0.8024 (6)	0.6571 (5)	−0.1054 (6)
C6	0.9920 (6)	0.7040 (5)	0.1896 (7)
C7	1.0867 (6)	0.6417 (6)	0.1852 (8)
C8	1.0306 (8)	0.7693 (5)	0.3125 (8)
C9	0.7900 (5)	0.6998 (4)	0.5282 (6)
C10	0.6931 (6)	0.7611 (5)	0.5386 (8)
C11	0.8898 (6)	0.7556 (5)	0.5613 (8)
C12	0.6293 (6)	0.5786 (5)	0.3411 (9)
C13	0.5965 (7)	0.5138 (7)	0.217 (1)
C14	0.6394 (7)	0.5291 (5)	0.457 (1)
C15	0.2039 (5)	−0.2242 (4)	−0.1903 (6)
C16	0.2138 (5)	−0.1935 (4)	−0.3099 (6)
C17	0.0951 (4)	−0.0815 (4)	−0.0717 (6)
C18	0.0436 (5)	−0.0326 (4)	−0.1963 (7)
C19	0.0153 (5)	−0.1462 (5)	−0.0642 (7)
C20	0.2713 (6)	−0.1971 (5)	0.0927 (7)
C21	0.3707 (6)	−0.2608 (5)	0.1154 (8)
C22	0.2889 (7)	−0.1321 (6)	0.2151 (7)
C23	0.2895 (6)	−0.0687 (4)	−0.4263 (6)
C24	0.1991 (7)	0.0033 (5)	−0.4350 (7)
C25	0.3875 (7)	−0.0297 (5)	−0.4384 (7)
C26	0.4438 (5)	−0.2061 (4)	−0.2780 (7)
C27	0.4173 (6)	−0.2658 (5)	−0.4087 (7)
C28	0.4836 (6)	−0.2646 (5)	−0.1642 (7)

Table IV. Selected Bond Distances (Å) and Angles (deg) in $[CrCl_2(dippe)]_2$

Bond Distances			
Cr1–ClA	2.381 (2)	Cr2–ClC	2.379 (2)
Cr1···ClA′	2.623 (2)	Cr2–ClC′	2.589 (2)
Cr1–ClB	2.332 (2)	Cr2–ClD	2.335 (2)
Cr1–P1	2.448 (2)	Cr2–P3	2.474 (2)
Cr1–P2	2.507 (2)	Cr2–P4	2.516 (2)
Cr1···Cr1′	3.640 (1)	Cr2···Cr2′	3.571 (1)
P1–C1	1.834 (8)	P3–C15	1.826 (7)
P1–C3	1.829 (6)	P3–C17	1.825 (6)
P1–C6	1.817 (7)	P3–C20	1.838 (6)
P2–C2	1.833 (7)	P4–C16	1.826 (6)
P2–C9	1.818 (7)	P4–C23	1.848 (6)
P2–C12	1.826 (7)	P4–C26	1.824 (6)
C1–C2	1.327 (1)[a]	C15–C16	1.515 (8)
Bond Angles			
ClA–Cr1–ClA′	86.78 (5)	ClC–Cr2–ClC′	88.20 (5)
ClA–Cr1–ClB	94.61 (6)	ClC–Cr2–ClD	94.10 (6)
ClA′–Cr1–ClB	99.58 (6)	ClC′–Cr2–ClD	101.08 (6)
P1–Cr1–P2	80.73 (6)	P3–Cr2–P4	80.96 (5)
ClA–Cr1–P1	169.85 (6)	ClC–Cr2–P3	169.27 (6)
ClA–Cr1–P2	91.65 (5)	ClC–Cr2–P4	91.82 (5)
ClA′–Cr1–P1	101.85 (6)	ClC′–Cr2–P3	101.29 (5)
ClA′–Cr1–P2	107.44 (5)	ClC′–Cr2–P4	105.04 (5)
ClB–Cr1–P1	89.26 (6)	ClD–Cr2–P3	89.02 (6)
ClB–Cr1–P2	152.55 (7)	ClD–Cr2–P4	153.37 (7)

[a] Shortened by disorder.

---

(26) Venkateswarlu, P. *J. Chem. Phys.* **1951**, *19*, 293.

(27) Cotton, F. A.; Rice, C. E.; Rice, G. W. *Inorg. Chim. Acta* **1977**, *24*, 231.

that are associated in the solid state. The bridging chlorides bridge asymmetrically, with long axial Cr···Cl distances of 2.623 (2) Å [2.589 (2) Å in molecule 2] and shorter Cr–Cl contacts to the other chromium center of 2.381 (2) Å. The terminal Cr–Cl distances of 2.332 (2) Å are shorter still, as expected, and are similar to the bond lengths of 2.348 (3) and 2.336 (2) Å in $CrCl_2(dmpe)_2$[16] and $CrCl_2(\eta^2\text{-tripod})_2$,[28] where tripod is 1,1,1-tris((dimethylphosphino)methyl)ethane.

The chromium–phosphorus distances are slightly different, with the shorter Cr–P contact of 2.488 (2) Å being trans to the semibridging chloride and the longer contact of 2.507 (2) Å being trans to the terminal chloride. This difference is small but entirely consistent with the different trans influences expected. The Cr–P distances are longer than those of low-spin chromium(II) phosphine complexes, which range from 2.342 (1) Å in $CrMe_2(dmpe)_2$[16] to 2.460 (1) Å in $Cr_2(CH_2SiMe_3)_4(PMe_3)_2$.[29-30]

The Cr···Cr separations are 3.640 (1) and 3.571 (1) Å in the two independent dimers and indicate that no metal–metal bonds are present. The $[CrCl_2(dippe)]_2$ dimer is the first chromium(II) representative of the $M_2Cl_4(PR_3)_4$ class of molecules, which in the molybdenum(II) and tungsten(II) systems adopt quadruply bonded structures.[31] Although the existence of $[Cr_2Me_8^{4-}]$[32,33] and molecular orbital calculations on $[Cr_2Cl_8^{4-}]$[34] suggest that the quadruply bonded dichromium configuration can contribute significantly to the ground state, the absence of strong metal–metal bonding in $[CrCl_2(dippe)]_2$ is consistent with the tendency of chromium(II) to form quadruple bonds only when supported by "three-atom" bridging ligands such as carboxylates, 2-hydroxypyridinates, and the like.[31] In the present case, the bulky dippe ligands may also prevent close approach of the two chromium centers.

Manganese(II). Manganese(II) bromide and iodide react with dippe at room temperature in toluene to yield $MnBr_2(dippe)$ and $MnI_2(dippe)$. Reaction of dippe with manganese(II) chloride under the same conditions yields only small amounts of $MnCl_2(dippe)$; however, higher yields of $MnCl_2(dippe)$ may be obtained by heating $MnCl_2$ in neat dippe at 70 °C for 12 h.

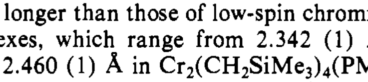

3a, X = Cl
b, X = Br
c, X = I

These pale-colored complexes are examples of tetrahedral, high-spin manganese(II), as shown by their solution magnetic moments of 5.7 μ_B in dichloromethane and by their EPR spectra as frozen glasses in toluene/dichloromethane. The latter contained features near 160 mT that are characteristic of rhombically distorted $S = {}^5/_2$ species.[35] In addition, a weak low-field transition at ca. 70 mT showed hyperfine coupling of 0.0072 cm^{-1} to the ^{55}Mn nucleus. No hyperfine splittings due to ^{31}P or ^1H nuclei were detected, indicating localization of the spin density on the manganese atom. Unfortunately, the higher field (>300 mT) components expected for high-spin manganese(II) were not sufficiently well-defined to allow exact assignment of the Hamiltonian parameters D and λ,[35] although the width of the 160 mT band is consistent with a symmetry parameters λ of near 0.3, as expected for a rhombically distorted ligand field.

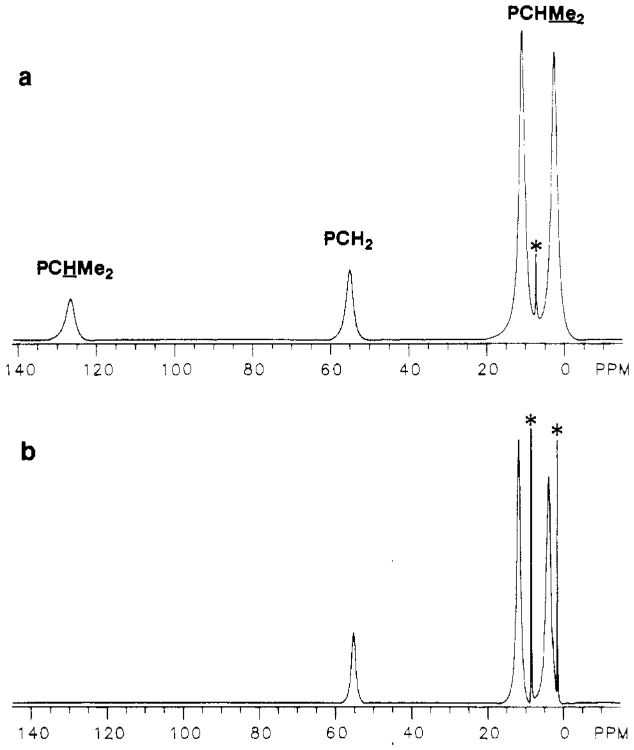

Figure 2. ^1H NMR spectra of $FeCl_2(dippe)$ (**4a**) in C_6D_6 at 25 °C: (a) unlabeled; (b) labeled with deuterium at the methine positions of the isopropyl groups, $FeCl_2[(CDMe_2)_2PCH_2CH_2P(CDMe_2)_2]$. Asterisks indicate peaks due to solvent and trace amounts of free dippe. A baseline-corrected spectrum is shown.

Other monomeric, high-spin MnX_2L_2 species have been described, including the halo species $MnI_2(PEt_3)_2$[36] and alkyl derivatives such as $Mn(CH_2CMe_2Ph)_2(PMe_3)_2$[35] and $Mn(t\text{-}Bu)_2(dmpe)$.[37] Other phosphine adducts of manganese(II) halides have been reported that do not adopt monomeric, four-coordinate structures: among these are the octahedral species $MnX_2(dmpe)_2$[16] and $MnCl_2(dmpb)_2$[38] [dmpb = 1,2-bis(dimethylphosphino)benzene] and the infinite polymer $[MnI_2(PMe_2Ph)]_n$.[39]

Iron(II). Ferrous halides readily react with dippe in toluene to give the adducts $FeX_2(dippe)$.[40]

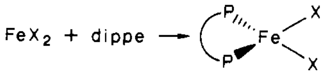

4a, X = Cl
b, X = Br
c, X = I

The colors become more intense from the chloride (pale lavender) through the bromide (orange-brown) to the iodide (olive green). Magnetic susceptibility measurements in solution establish a high-spin electronic configuration for all these complexes; the magnetic moments of 4.9–5.0 μ_B are near the spin-only value of 4.90 μ_B for four unpaired electrons.

Despite the fact that the $FeX_2(dippe)$ derivatives are paramagnetic, ^1H NMR resonances are readily observable. The ^1H NMR spectrum of $FeCl_2(dippe)$ exhibits broad, highly shifted resonances (Figure 2a) due to the presence on the iron center of four unpaired electrons. The peak assignments have been made

---

(28) Arif, A. M.; Hefner, J. G.; Jones, R. A.; Whittlesey, B. R. *Inorg. Chem.* **1986**, *25*, 1080.

(29) Andersen, R. A.; Jones, R. A.; Wilkinson, G. *J. Chem. Soc., Dalton Trans.* **1978**, 446.

(30) Hursthouse, M. B.; Malik, K. M. A. *J. Chem. Soc., Dalton Trans.* **1978**, 1314.

(31) Cotton, F. A.; Walton, R. A. *Multiple Bonds Between Metal Atoms*; Wiley: New York, 1982.

(32) Kurras, E.; Otto, J. *J. Organomet. Chem.* **1965**, *4*, 114.

(33) Krause, J.; Marx, G.; Schödl, G. *J. Organomet. Chem.* **1970**, *21*, 159.

(34) Benard, M. *J. Am. Chem. Soc.* **1978**, *100*, 2354.

(35) Howard, C. G.; Girolami, G. S.; Wilkinson, G.; Thornton-Pett, M.; Hursthouse, M. B. *J. Chem. Soc., Dalton Trans.* **1983**, 2631.

(36) Hebendanz, N.; Kohler, F. H.; Müller, G. *Inorg. Chem.* **1984**, *23*, 3043.

(37) Girolami, G. S.; Howard, C. G.; Wilkinson, G.; Dawes, H. M.; Thornton-Pett, M.; Motevalli, M.; Hursthouse, M. B. *J. Chem. Soc., Dalton Trans.* **1985**, 921.

(38) Warren, L. F.; Bennett, M. A. *Inorg. Chem.* **1976**, *15*, 3126.

(39) Beagley, B.; Briggs, J. C.; Hosseiny, A.; Hill, W. E.; King, T. J.; McAuliffe, C. A.; Minten, K. *J. Chem. Soc., Chem. Commun.* **1984**, 305.

(40) Professor M. Fryzuk of the University of British Columbia has also prepared $FeCl_2(dippe)$. We thank him for communicating this result to us.

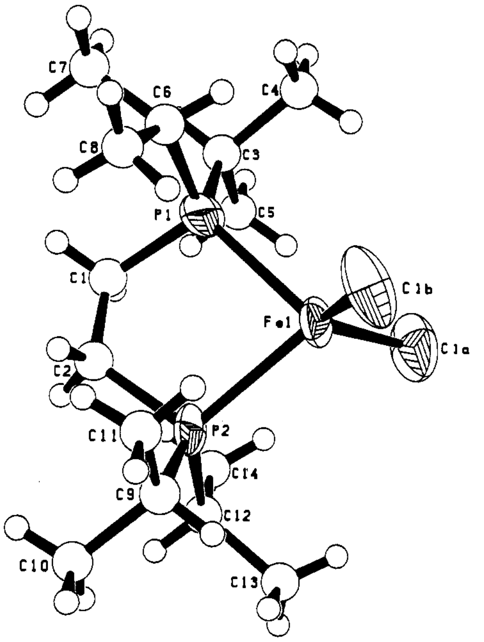

Figure 3. Molecular structure of $FeCl_2$(dippe). Molecule 1 is shown; molecule 2 adopts an essentially identical structure.

on the basis of integrated intensities and a labeling study. In order to distinguish the resonances for the dippe methylene and methine protons (which have the same integrated intensity), complex **4a** was specifically deuteriated at the methine, P*CD*Me_2, position. The ^1H NMR spectrum of $FeCl_2$(dippe-d_4) lacks a resonance at δ 126 (Figure 2b), so the resonances at δ 126 and 55 in the protio derivative can be assigned to the methine and methylene protons, respectively.

Iron(II) is only rarely found to be four-coordinate.[41] Perhaps the most important example of this geometry is the tetrahedral iron(II) center found in the reduced form of rubredoxin, an iron-containing protein in which the iron atom is coordinated to four cysteine sulfur atoms.[42,43] Molecular examples of tetrahedral iron(II) include salts of the [$FeCl_4^{2-}$] anion,[44] [FeL_4^{2+}] complexes where L is Ph_3PO or $(Me_2N)_3PO$,[45,46] some rubredoxin analogues with FeS_4 donor ligand sets,[47,48] and a few other complexes. Although complexes of stoichiometry $FeCl_2(PR_3)_2$ have been reported previously, proof of their monomeric nature is largely lacking.[49–51]

In order to detemine the molecular parameters of $FeCl_2$(dippe), its X-ray crystal structure has been determined; these results reveal a monomeric, four-coordinate geometry in the solid state (Figure 3). Crystallographic data and selected bond lengths and angles are collected in Tables II, V, and VI. The weak crystal diffraction pattern, the diffuse scatter, and the high thermal coefficients for the terminal carbon atoms probably indicate significant disorder in these positions. These considerations limit the precision of the structural parameters and reduce the number of conclusions that may be safely drawn; nevertheless, the overall coordination geometry is well-defined and the important features of the structure are unambiguously determined.

Table V. Final Atomic Coordinates for $FeCl_2$(dippe)

	x/a	y/b	z/c
Fe1	0.2246 (2)	0.0200 (2)	0.3365 (3)
Fe2	0.0133 (2)	0.2222 (2)	0.3748 (3)
ClA	0.2790 (5)	0.0912 (4)	0.2887 (6)
ClB	0.1684 (5)	−0.0213 (6)	0.2386 (6)
ClC	−0.0075 (5)	0.1540 (4)	0.4749 (6)
ClD	0.0702 (4)	0.2905 (5)	0.4182 (6)
P1	0.2744 (5)	−0.0557 (5)	0.4219 (6)
P2	0.1830 (4)	0.0424 (4)	0.4822 (5)
P3	−0.0639 (4)	0.2644 (5)	0.2991 (6)
P4	0.0343 (4)	0.1806 (4)	0.2275 (5)
C1	0.261 (2)	−0.042 (2)	0.537 (3)
C2	0.211 (2)	−0.014 (2)	0.558 (2)
C3	0.344 (2)	−0.061 (2)	0.416 (3)
C4	0.361 (2)	−0.078 (2)	0.319 (3)
C5	0.371 (2)	−0.004 (2)	0.448 (3)
C6	0.254 (2)	−0.133 (2)	0.397 (3)
C7	0.276 (2)	−0.180 (2)	0.453 (3)
C8	0.197 (3)	−0.153 (3)	0.409 (4)
C9	0.112 (2)	0.039 (2)	0.490 (3)
C10	0.087 (2)	0.051 (2)	0.587 (3)
C11	0.090 (2)	−0.020 (2)	0.457 (3)
C12	0.203 (2)	0.118 (2)	0.532 (3)
C13	0.177 (2)	0.171 (2)	0.474 (3)
C14	0.257 (2)	0.120 (2)	0.539 (3)
C15	−0.055 (2)	0.251 (2)	0.182 (3)
C16	−0.017 (2)	0.209 (2)	0.152 (2)
C17	−0.077 (2)	0.340 (2)	0.297 (3)
C18	−0.081 (2)	0.360 (2)	0.390 (3)
C19	−0.032 (2)	0.373 (2)	0.257 (3)
C20	−0.134 (3)	0.230 (3)	0.335 (5)
C21	−0.173 (3)	0.252 (3)	0.271 (5)
C22	−0.130 (4)	0.190 (3)	0.350 (6)
C23	0.032 (2)	0.099 (2)	0.223 (3)
C24	0.034 (2)	0.076 (2)	0.119 (3)
C25	−0.021 (2)	0.069 (2)	0.258 (3)
C26	0.095 (2)	0.201 (2)	0.178 (3)
C27	0.144 (2)	0.177 (2)	0.225 (3)
C28	0.104 (2)	0.271 (2)	0.170 (3)

Table VI. Selected Bond Distances (Å) and Angles (deg) in $FeCl_2$(dippe)

	Bond Distances		
Fe1–ClA	2.22 (1)	Fe2–ClC	2.21 (1)
Fe1–ClB	2.23 (1)	Fe2–ClD	2.29 (1)
Fe1–P1	2.47 (1)	Fe2–P3	2.42 (1)
Fe1–P2	2.466 (9)	Fe2–P4	2.456 (9)
P1–C1	1.79 (4)	P3–C15	1.79 (5)
P1–C3	1.73 (5)	P3–C17	1.76 (5)
P1–C6	1.87 (4)	P3–C20	1.98 (8)
P2–C2	1.84 (4)	P4–C16	1.81 (4)
P2–C9	1.75 (4)	P4–C13	1.86 (4)
P2–C12	1.94 (4)	P4–C26	1.74 (4)
C1–C2	1.43 (6)	C15–C16	1.42 (6)
	Bond Angles		
ClA–Fe1–ClB	118.0 (4)	ClC–Fe2–ClD	116.2 (4)
P1–Fe1–P2	83.7 (3)	P3–Fe2–P4	84.0 (3)
ClA–Fe1–P1	111.9 (5)	ClC–Fe2–P3	114.3 (4)
ClA–Fe1–P2	112.9 (4)	ClC–Fe2–P4	113.0 (4)
ClB–Fe1–P1	111.0 (4)	ClD–Fe2–P3	111.4 (4)
ClB–Fe1–P2	114.3 (4)	ClD–Fe2–P4	113.8 (4)

Two independent molecules of $FeCl_2$(dippe) are contained in the asymmetric unit. The two molecules are virtually identical, and the following discussion will refer to molecule 1, since it is less affected by disorder. Although the compound possesses no crystallographically imposed symmetry, overall it possesses approximate C_s symmetry due to the disposition of the isopropyl substituents of the dippe ligand. Two of the isopropyl methine protons (those on C6 and C9) are directed roughly toward the $FeCl_2$ unit, while the remaining methine protons (on C3 and C12) are directed away from this unit. Undoubtedly this arrangement minimizes nonbonded repulsions among the isopropyl groups. If one neglects the isopropyl substituents, the iron center adopts a distorted-tetrahedral geometry of approximate C_{2v} symmetry. The

---

(41) Cotton, F. A.; Wilkinson, G. *Advanced Inorganic Chemistry*, 4th ed.; Wiley: New York, 1980; Chapter 21-E-4.

(42) Watenpaugh, K. D.; Sieker, L. C.; Jensen, L. H. *J. Mol. Biol.* **1979**, *131*, 509.

(43) Shulman, R. G.; Eisenberger, P.; Teo, B. K.; Kincaid, B. M.; Brown, G. S. *J. Mol. Biol.* **1978**, *124*, 305.

(44) Lauher, J. W.; Ibers, J. A. *Inorg. Chem.* **1975**, *14*, 348.

(45) Donoghue, J. T.; Drago, R. S. *Inorg. Chem.* **1963**, *2*, 1158.

(46) Foster, D.; Goodgame, D. M. L. *J. Chem. Soc.* **1965**, 268. See also p 454.

(47) Churchill, M. R.; Wormald, J. *Inorg. Chem.* **1971**, *10*, 1778.

(48) Lane, R. W.; Ibers, J. A.; Frankel, R. B.; Papaefthymiou, G. C.; Holm, R. H. *J. Am. Chem. Soc.* **1977**, *99*, 84.

(49) Booth, G.; Chatt, J. *J. Chem. Soc.* **1962**, 2099.

(50) Baker, W. A.; Lutz, P. M. *Inorg. Chim. Acta* **1976**, *16*, 5.

(51) Pignolet, L. H.; Forster, D.; Horrocks, W. D. *Inorg. Chem.* **1968**, *7*, 828.

dihedral angle between the Cl–Fe–Cl and P–Fe–P planes of 88.3° is very near the idealized value of 90°. In the closely related *p*-methylbenzyl derivative $Fe(CH_2C_6H_4Me)_2$(dippe), the corresponding value for this dihedral angle was 85°.[6] The Cl–Fe–Cl and P–Fe–P angles in $FeCl_2$(dippe) of 118.0 (4) and 83.7 (3)° are also similar to the corresponding values of 111.8 (2) and 83.33 (7)° in the *p*-methylbenzyl complex.[6]

The average Fe–Cl distance of 2.22 (1) Å in $FeCl_2$(dippe) is significantly shorter than the Fe–Cl bond lengths of 2.35 Å in the octahedral molecules of $FeCl_2(dmpe)_2$, $FeCl_2(depe)_2$, $FeCl_2(dppen)_2$, and $FeCl_2(triphos)_2$,[52,53] where depe = $Et_2PCH_2CH_2PEt_2$, dppen = $Ph_2PCH{=}CHPPh_2$, and triphos = $(Ph_2PCH_2CH_2)_2PPh$. A more appropriate comparison is with the high-spin tetrahedral $[FeCl_4{}^{2-}]$ anion, which exhibits Fe–Cl bond lengths of 2.29 Å.[44] The $FeCl_2$(dippe) molecule thus possesses very short Fe–Cl bonds even in comparison with other tetrahedral iron(II) species.

The Fe–P bond lengths of 2.47 (1) Å are essentially identical with those in the related high-spin iron alkyl $Fe(CH_2C_6H_4Me)_2$(dippe) of 2.462 (2) Å.[6] As noted previously, the values are intermediate between the 2.24–2.30 Å distances reported for octahedral low-spin iron(II) species and the 2.53–2.71 Å distances found in octahedral high-spin complexes.[52,53] These variations were attributed to the differing coordination numbers and the significant decrease in π-back-bonding with the phosphorus ligands in high-spin compounds.[6]

Cobalt(II). Reaction of anhydrous $CoCl_2$ with dippe in diethyl ether gives a green solid, which may be purified by Soxhlet extraction with diethyl ether. Blue-green $CoCl_2$(dippe) adopts a monomeric tetrahedral structure like that of $FeCl_2$(dippe). The solid-state IR spectra of $CoCl_2$(dippe) and $FeCl_2$(dippe) are virtually identical, with the Co–Cl stretches falling in the terminal M–Cl region. The magnetic moment of 3.9 μ_B, indicative of a high-spin d^7 system, is also consistent with a tetrahedral structure; square-planar Co^{II} molecules are invariably low spin with only one unpaired electron.[54-56]

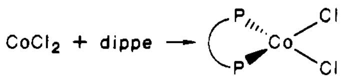

5

Concluding Remarks. The electron-donating phosphine 1,2-bis(diisopropylphosphino)ethane has allowed us to prepare a new series of related adducts, MX_2(dippe), of the first-row transition metals. The steric and electronic properties of this chelating phosphine have been tailored to allow the formation of monoadducts, with no evidence of diadduct formation analogous to the $MX_2(dmpe)_2$ complexes[16] being noted. Accordingly, the MX_2(dippe) species possess reduced coordination numbers and electron counts; the high degree of coordinative and electronic unsaturation makes these complexes of particular interest.

Physical data reveal that, with the exception of the vanadium(II) species, each complex adopts a four-coordinate structure that in one case, chromium(II), is loosely associated in the solid state. The d^4 chromium compounds show a preference for square-planar geometries unlike the tetrahedral manganese, iron, and cobalt analogues; this preference is electronic in origin and reflects the enhanced stabilization energy attained upon half-filling the four low-lying d orbitals characteristic of square-planar ligand arrays. All of the MX_2(dippe) species adopt high-spin electronic configurations.

The MX_2(dippe) complexes provide a homologous series in which to compare the behavior of coordinately unsaturated first-row transition-metal species. We have shown that they serve as excellent starting materials for the preparation of novel organometallic derivatives of these elements: for example, 12-electron chromium(II) alkyls, CrR_2(dippe), and 14-electron iron(II) alkyls, FeR_2(dippe), are readily obtained upon alkylation of the dihalo species with Grignard or dialkylmagnesium reagents.[6,12] Such low-electron metal alkyls are of great interest in terms of their relationship to catalysts for the polymerization of olefins. Further studies of the MX_2(dippe) species as synthetic entries to the organometallic chemistry of the first-row transition elements are under way.

Experimental Section

All operations were carried out under vacuum or under argon. Solvents were distilled under nitrogen from sodium (toluene) or sodium-benzophenone (pentane, diethyl ether, tetrahydrofuran) immediately before use.

1,2-Bis(diisopropylphosphino)ethane[57] was prepared via a literature route. Isopropyl-d_1 chloride (MSD Isotopes) was used to prepare dippe selectively labeled at the methine positions, $(CDMe_2)_2PCH_2CH_2P(CDMe_2)_2$. Anhydrous VBr_3 was converted to $VBr_3(thf)_3$[58] by a literature route; $CrCl_2$(thf)[59] and $MnBr_2$[60] were prepared from the metal and anhydrous HX in tetrahydrofuran and diethyl ether, respectively, while MnI_2[61] was prepared from Mn metal and I_2 in diethyl ether. Anhydrous $FeCl_2$ was obtained by refluxing $FeCl_3$ in chlorobenzene,[62] and $FeBr_2$ and FeI_2 were obtained by dissolving high-purity iron wire in the corresponding mineral acid and dehydrating the product by heating under vacuum.[63] Anhydrous $CoCl_2$ was prepared by action of $SOCl_2$ on the hydrate followed by drying under vacuum.

Microanalyses were performed by Josef Nemeth and Thomas McCarthy of the University of Illinois Microanalytical Laboratory. The IR spectra were recorded as Nujol mulls on a Perkin-Elmer 599B using KBr plates unless otherwise noted. The ^1H NMR data were recorded on a Perkin-Elmer R24-B instrument at 60 MHz or on a General Electric QE-300 at 300 MHz. The NMR data were obtained in C_6D_6 (δ 7.15), and chemical shifts are uncorrected for the paramagnetic shift of the solvent. The X-band EPR experiments were performed on a Varian E-9 with frozen toluene/dichloromethane solutions at −196 °C. Magnetic moments were determined by a modification of Evans' method.[64] Melting points were determined on a Thomas-Hoover Unimelt apparatus in closed capillaries under argon.

1. Dibromo[1,2-bis(diisopropylphosphino)ethane]vanadium(II)-1.5-(Tetrahydrofuran) (1). To a solution of $VBr_3(thf)_3$ (0.81 g, 1.60 mmol) in tetrahydrofuran (30 mL) were added dippe (0.5 mL, 1.75 mmol) and Mg powder (0.04 g, 1.67 mmol). The solution initially turned dark orange and after being refluxed for 3 h turned bright green. The solution was filtered while warm and cooled to −20 °C, yielding a green crystalline solid. Yield: 0.57 g (61%). IR (cm^{-1}): 1631 m, 1411 s, 1339 w, 1293 m, 1253 m, 1220 w, 1158 w, 1110 w, 1091 w, 1059 s, 1031 s, 956 w, 918 s, 881 s, 848 s, 819 m, 755 w, 716 w, 683 m, 666 s, 631 s, 509 m, 466 w, 426 w.

2. Tetrachlorobis[1,2-bis(diisopropylphosphino)ethane]dichromium(II) (2a). To a suspension of $CrCl_2$(thf) (0.73 g, 3.7 mmol) in diethyl ether (30 mL) was added dippe (1.1 mL, 3.9 mmol). The solution immediately turned pale blue, and a blue solid formed. The solid was filtered off, washed with diethyl ether (20 mL), and dried under vacuum. Yield: 0.87 g (61%). The solid can be recrystallized from hot toluene to give X-ray-quality crystals. IR (cm^{-1}, CsI): 2716 w, 1409 m, 1334 s, 1297 m, 1241 s, 1156 m, 1097 m, 1032 s, 964 w, 925 m, 856 w, 846 w, 795 m, 721 w, 691 s, 680 s, 664 s, 621 w, 608 w, 491 w, 462 w, 443 w, 381 w, 300 s (Cr–Cl), 270 s (Cr–Cl).

3. Tetrabromobis[1,2-bis(diisopropylphosphino)ethane]dichromium(II) (2b). To a suspension of $CrBr_2(thf)_2$ (0.63, 1.8 mmol) in diethyl ether (30 mL) was added dippe (0.6 mL, 2.1 mmol). The solution turned blue, and a blue solid formed. After the mixture was stirred for 3 h, the solvent was removed by filtration, and the blue solid was washed with diethyl ether (10 mL) and dried under vacuum. Yield: 0.58 g (68%). IR

---

(52) DiVaira, M.; Midollini, S.; Sacconi, L. *Inorg. Chem.* **1981**, *20*, 3430.
(53) Cecconi, F.; DiVaira, M.; Midollini, S.; Sacconi, L. *Inorg. Chem.* **1981**, *20*, 3423.
(54) Cotton, F. A.; Faust, O. D.; Goodgame, D. M. L.; Holm, R. H. *J. Am. Chem. Soc.* **1961**, *83*, 1780.
(55) Horrocks, W. D.; Greenberg, E. S. *Inorg. Chem.* **1971**, *10*, 2190.
(56) Horrocks, W. D.; Van Hecke, G. R.; Hall, D. W. *Inorg. Chem.* **1967**, *6*, 694.
(57) Fryzuk, M. D.; Jones, T.; Einstein, F. W. B. *Organometallics* **1984**, *3*, 185.
(58) Fowles, G. W. A.; Green, P. T.; Lester, T. E. *J. Inorg. Nucl. Chem.* **1967**, *29*, 2365.
(59) Larkworthy, L. F.; Nelson-Richardson, M. H. O. *Chem. Ind. (London)* **1974**, 164.
(60) Hermes, A. R., unpublished results.
(61) Ducelliez, F. *Bull. Soc. Chim. Fr.* **1913**, [4]*13*, 815.
(62) Kovacic, P.; Brace, N. O. *Inorg. Synth.* **1960**, *6*, 172.
(63) Winter, G. *Inorg. Synth.* **1973**, *14*, 101.
(64) Evans, D. F.; Fazakerley, G. V.; Phillips, R. F. *J. Chem. Soc. A* **1971**, 1931.

(cm^{-1}): 1413 m, 1295 w, 1248 m, 1162 m, 1100 w, 1082 w, 1039 s, 970 w, 931 m, 890 s, 862 s, 796 m, 729 w, 700 s, 683 s, 669 m, 623 w, 479 w.

4. **Dibromo[1,2-bis(diisopropylphosphino)ethane]chromium(II)–Acetonitrile.** [CrBr$_2$(dippe)]$_2$ (0.50 g, 0.5 mmol) was dissolved in acetonitrile (20 mL). The deep blue solution was filtered and concentrated to ca. 5 mL. Cooling to −20 °C resulted in the formation of large blue crystals. Yield: 0.40 g (74%). IR (cm^{-1}): 2700 w, 2313 w, 2278 w, 1424 s, 1311 m, 1267 m, 1261 s, 1184 m, 1129 w, 1114 m, 1063 m, 1044 s, 979 w, 949 m, 911 s, 874 m, 823 m, 746 m, 712 s, 705 s, 663 w, 652 m, 628 w, 606 w, 513 w, 490 w.

5. **Dichloro[1,2-bis(diisopropylphosphino)ethane]manganese(II) (3a).** MnCl$_2$ (0.43 g, 3.4 mmol) and dippe (1.5 mL, 5.3 mmol) were combined and heated to ca. 70 °C for 12 h. The resulting tan solid was extracted with hot toluene (30 mL), and pale green prisms were obtained after filtering the solution and cooling to −20 °C. Yield: 0.30 g (23%). IR (cm^{-1}, CsI): 2724 w, 1422 m, 1416 m, 1305 w, 1290 w, 1244 s, 1160 m, 1139 m, 1112 w, 1088 w, 1076 w, 1051 w, 1032 w, 1023 m, 924 m, 888 s, 859 s, 824 m, 727 m, 692 s, 680 s, 667 s, 639 w, 622 m, 474 m, 427 w, 298 s (Mn–Cl), 250 s (Mn–Cl).

6. **Dibromo[1,2-bis(diisopropylphosphino)ethane]manganese(II) (3b).** To a suspension of MnBr$_2$ (0.60 g, 2.8 mmol) in toluene (30 mL) was added dippe (0.8 mL, 2.8 mmol). After being stirred for 24 h, the pale pink suspension was warmed to 60 °C to dissolve most of the solid, and the solution was filtered while hot. Cooling to −20 °C resulted in the formation of pale green crystals. Yield: 0.98 g (73%). IR (cm^{-1}): 2758 w, 1423 m, 1417 m, 1368 s, 1298 w, 1256 s, 1160 m, 1113 w, 1076 w, 1048 w, 1032 m, 1025 sh, 963 w, 922 m, 888 m, 880 sh, 860 m, 825 w, 737 m, 691 m, 680 s, 667 m, 620 w, 433 w.

7. **Diiodo[1,2-bis(diisopropylphosphino)ethane]manganese(II) (3c).** To a suspension of MnI$_2$ (1.46 g, 4.7 mmol) in toluene (60 mL) was added dippe (1.3 mL, 4.7 mmol). After being stirred for 24 h, the tan suspension was heated to ca. 75 °C and the orange solution was filtered while hot. Pale orange needles of the toluene solvate MnI$_2$(dippe)·C$_7$H$_8$ crystallized immediately upon cooling the solution to room temperature. Yield: 2.3 g (86%). IR (cm^{-1}): 2717 w, 1407 m, 1297 w, 1260 w, 1237 s, 1160 m, 1112 w, 1082 w, 1046 sh, 1031 s, 962 w, 927 m, 882 m, 852 m, 800 w, 727 m, 681 s, 634 w, 614 w, 467 w.

8. **Dichloro[1,2-bis(diisopropylphosphino)ethane]iron(II) (4a).** To a suspension of FeCl$_2$ (2.16 g, 17.0 mmol) in toluene (50 mL) was added dippe (4.9 mL, 17.2 mmol). After the suspension was stirred for 4 h, the solid dissolved, and the pale orange solution was filtered, concentrated to ca. 20 mL, and cooled to −20 °C, yielding lavender needles. An additional crop of crystals was obtained by concentrating and cooling the supernatant. Yield: 5.6 g (85%). IR (cm^{-1}, CsI): 2723 w, 1412 m, 1388 s, 1370 s, 1298 w, 1260 w, 1241 s, 1160 m, 1139 w, 1110 m, 1098 w, 1078 w, 1047 w, 1032 s, 965 w, 941 m, 886 s, 853 m, 806 m, 793 sh, 723 w, 688 s, 647 w, 619 m, 468 w, 430 w, 358 s (Fe–Cl), 318 s (Fe–Cl).

The complex selectively deuteriated at the methine positions of the isopropyl groups was prepared similarly from the appropriately labeled dippe phosphine.

9. **Dibromo[1,2-bis(diisopropylphosphino)ethane]iron(II) (4b).** To a suspension of FeBr$_2$ (0.64 g, 3.0 mmol) in toluene (30 mL) was added dippe (0.9 mL, 3.1 mmol). The solid dissolved immediately, giving an orange-brown solution. The filtered solution was concentrated to ca. 15 mL and cooled to −20 °C to give large orange-brown prisms. Additional crops of crystals were obtained from the supernatant. Yield: 1.22 g (87%). IR (cm^{-1}, CsI): 2704 w, 1404 m, 1379 s, 1362 s, 1290 w, 1250 sh, 1232 s, 1151 m, 1129 sh, 1101 m, 1089 w, 1069 m, 1039 m, 1022 s, 954 w, 921 s, 874 s, 849 m, 839 sh, 800 m, 784 w, 714 w, 669 s, 624 w, 610 m, 471 w, 424 w, 272 s (Fe–Br).

10. **Diiodo[1,2-bis(diisopropylphosphino)ethane]iron(II) (4c).** To a suspension of FeI$_2$ (1.2 g, 3.9 mmol) in toluene (30 mL) was added dippe (1.1 mL, 3.9 mmol). The solid dissolved immediately, giving a dark orange-brown solution. The filtered solution was concentrated to ca. 15 mL and cooled to −20 °C, yielding olive green needles. Yield: 1.80 g (81%). IR (cm^{-1}): 2705 w, 1407 m, 1379 s, 1361 s, 1290 w, 1253 sh, 1239 s, 1154 m, 1132 w, 1104 m, 1085 w, 1042 m, 1027 s, 958 w, 924 s, 875 s, 854 m, 800 m, 790 sh, 687 sh, 673 s, 649 m, 608 m, 480 w, 450 w.

11. **Dichloro[1,2-bis(diisopropylphosphino)ethane]cobalt(II) (5).** To a suspension of CoCl$_2$ (0.84 g, 6.5 mmol) in diethyl ether (25 mL) was added dippe (1.9 mL, 6.7 mmol). The solution turned green, and a green solid formed. The solvent was removed under vacuum, and the solid was washed with pentane (20 mL) and dried under vacuum. After being transferred to a Soxhlet extractor, the solid was extracted with diethyl ether for 8 h, resulting in a blue-green solution. Cooling the solution to −20 °C resulted in the formation of blue-green crystals. Yield: 0.73 g (28%). IR (cm^{-1}, CsI): 2700 w, 1408 m, 1303 w, 1289 w, 1243 s, 1163 s, 1115 m, 1101 m, 1081 m, 1051 sh, 1038 s, 967 w, 940 sh, 932 m, 890 s, 864 m, 854 m, 811 m, 797 m, 729 w, 688 s, 674 s, 648 w, 626 m, 483 m, 433 w, 385 s (Co–Cl), 321 s (Co–Cl).

Crystallographic Studies.[65] Single crystals of [CrCl$_2$(dippe)]$_2$ grown from toluene were sealed in thin-walled glass capillaries under argon. [Single crystals of FeCl$_2$(dippe) were also grown from toluene; subsequent comments in brackets will refer to this compound.] Preliminary photographs yielded rough cell dimensions, and a suitable crystal was transferred to the diffractometer. Standard peak search and automatic indexing procedures followed by least-squares refinement using 15 reflections yielded the cell dimensions given in Table II.

Data were collected in two quadrants [one octant] of reciprocal space ($\pm h,\pm k,+l$) [$+h,+k,+l$] with measurement parameters listed in Table II. The choice of centric space group $P\bar{1}$ was confirmed by successful refinement of the proposed model. [The systematic absences $0kl$ ($k \neq 2n$), $h0l$ ($l \neq 2n$), and $hk0$ ($h \neq 2n$) uniquely defined the space group *Pbca*.] The measured intensities were reduced to structure factor amplitudes and their estimated standard deviations by correction for background, scan speed, and Lorentz and polarization effects. Corrections for crystal decay and absorption were applied, the maximum and minimum transmission factors for the latter being 0.794 and 0.761 [0.756 and 0.712]. Questionable reflections, including 82 poorly centered peaks, were deleted. Only those data with $I > 2.58\sigma(I)$ were used in the least-squares refinement. [The crystal of FeCl$_2$(dippe) gave a weak diffraction pattern as shown by the low percentage of "observed" data.]

The structure was solved by direct methods (SHELX) [MULTAN] and subsequently by least-squares difference Fourier calculations. The quantity minimized by the least-squares program was $\sum w(|F_o - F_c|)^2$ where $w = 1.88/(\sigma(F_o)^2 + (pF_o)^2)$ [$w = 4.67/(\sigma(F_o)^2 + (pF_o)^2)$]. In the final cycle of least squares, non-hydrogen atoms were independently refined with anisotropic thermal coefficients. A group isotropic thermal parameter was varied for the hydrogen atoms, which were fixed in "idealized" positions (for methyl hydrogens, staggered with respect to the substituents on the attached sp^3 atom) with C–H = 0.95 Å. [In the final cycle of least squares, the iron, chlorine, and phosphorus atoms were refined with anisotropic thermal coefficients, carbon atoms were refined with isotropic coefficients (except C22), and a group isotropic thermal parameter was refined for the hydrogen atoms. The position for atom C22 was located in a difference Fourier map and fixed, while hydrogen atoms were included as fixed contributors in "idealized" positions with C–H = 0.95 Å (H20 and methyl hydrogen atoms H22 were not included).] Successful convergence was indicated by the maximum shift/error of 0.001 [0.10] for the last cycle. Final refinement parameters are given in Table II. The final difference Fourier map had no significant features. There were no apparent systematic errors between the final observed and calculated structure factors.

Acknowledgment. We thank the National Foundation (Grant CHE-85-21757) and the Office of Naval Research through their Young Investigator Award Program for support of this research and the Exxon Foundation for a fellowship (A.R.H.). G.S.G. is the recipient of a Sloan Foundation Research Fellowship (1988–1990). We particularly wish to thank Dr. Scott R. Wilson and Charlotte Stern of the University of Illinois X-ray Crystallographic Laboratory for performing the X-ray crystal structure determinations.

Supplementary Material Available: Tables of hydrogen atom coordinates, anisotropic thermal parameters, and complete bond distances and angles for [CrCl$_2$(dippe)]$_2$ and FeCl$_2$(dippe) (8 pages); a listing of final observed and calculated structure factors for [CrCl$_2$(dippe)]$_2$ and FeCl$_2$(dippe) (22 pages). Ordering information is given on any current masthead page.

---

(65) For further details of the programs and refinement procedures used, see: Jensen, J. A.; Wilson, S. R.; Girolami, G. S. *J. Am. Chem. Soc.*, in press.